

Band Structure and High-Field Transport Properties of InP

L. W. JAMES

Varian Associates, Central Research Laboratories, Palo Alto, California 94303

AND

J. P. VAN DYKE* AND F. HERMAN

IBM Research Laboratory, San Jose, California 95114

AND

D. M. CHANG

Hewlett-Packard Laboratory, Palo Alto, California 94303

(Received 3 December 1969)

Using the technique of energy-distribution analysis of photoemitted electrons, we have accurately located the position of several band-structure features of InP, including the next higher conduction-band minimum above the Γ_1 minimum at 1.95 eV above the valence-band maximum, independent of temperature. This minimum is tentatively associated with the L_1 symmetry point. High-temperature Hall-effect measurements confirm that there are no minima between the lowest two observed by photoemission. A band structure for InP has been computed using these new data in an empirically adjusted first-principles orthogonalized-plane-wave (OPW) calculation. The velocity-field characteristic has been calculated for a range of lattice temperatures. A negative differential mobility is predicted, with a room-temperature threshold field of 11 500 V/cm and a peak drift velocity of 3×10^7 cm/sec.

I. INTRODUCTION

ENERGY-DISTRIBUTION analysis of photoemitted electrons has proven to be a valuable tool in the determination of the details of the electronic band structure of materials. For GaAs, the Γ_1 , X_1 , L_1 , and X_3 conduction-band minima have been experimentally located^{1,2} providing enough experimental data for an

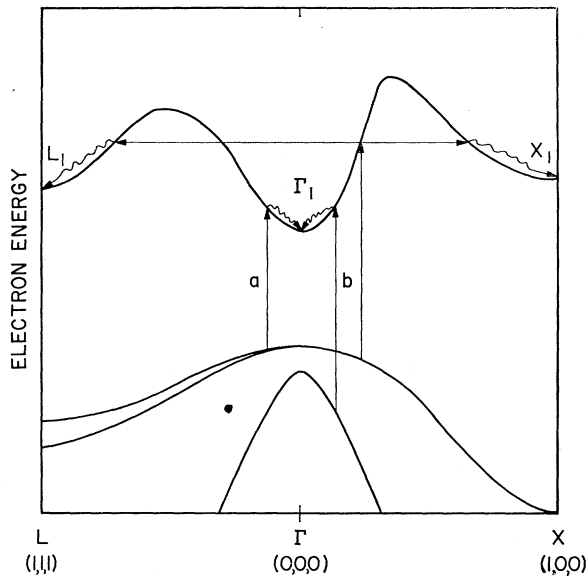


FIG. 1. InP band structure near the energy gap showing examples of photoexcitation, scattering, and thermalization; (a) represents a low-photon energy with all thermalization in Γ_1 , (b) represents a larger photon energy where scattering to the upper valleys and thermalization in them can occur.

* Present address: Sandia Laboratories, Albuquerque, N. M.

¹ R. C. Eden, J. L. Moll, and W. E. Spicer, Phys. Rev. Letters **13**, 597 (1967).

² L. W. James, R. C. Eden, J. L. Moll, and W. E. Spicer, Phys. Rev. **174**, 909 (1968).

accurate band-structure calculation.³ The temperature dependence of the location of the Γ_1 and X_1 minima has been determined,⁴ and the intervalley coupling parameters important in velocity-field calculations and in the frequency dependence of the Gunn effect have been determined.⁴

The Gunn effect has been observed in InP as well as GaAs.⁵ Uebbing and Bell showed that with a Cs-O surface layer, the vacuum level could be lowered below the lowest conduction-band minimum in p -type InP,⁶ making it possible to investigate InP in a manner similar to GaAs. Energy-distribution curves (EDC's) on InP were taken by Fischer,⁷ but he used n -type material, preventing the examination of structure near the band gap. We have taken high resolution EDC's on p -type InP with a Cs-O surface layer, allowing examination of conduction-band structure near the band gap, including the critical lower- to upper-valley energy separation.

II. EXPERIMENTAL METHODS

Single crystals of 5×10^{18} cm⁻³ p -type Zn-doped InP were cut from a polycrystalline ingot and mounted in an ultrahigh vacuum cleaving chamber with a $\langle 110 \rangle$ face parallel to the cleaving apparatus. Three-millimeter-square $\langle 110 \rangle$ faces were the largest single crystals in the ingot, limiting the EDC resolution to less than that obtained for GaAs⁴ due to the effect of fringing fields from the sides of the crystal which had higher work functions than the cleaved face.

³ F. Herman, R. L. Kortum, C. D. Kuglin, J. P. Van Dyke, and S. Skillman, *Methods of Computational Physics* (Academic, New York, 1968), Vol. 8.

⁴ L. W. James and J. L. Moll, Phys. Rev. **183**, 740 (1969).

⁵ J. B. Gunn, Solid State Commun. **1**, 88 (1963).

⁶ J. J. Uebbing and R. L. Bell, Proc. IEEE **56**, 1624 (1968).

⁷ T. E. Fisher, Phys. Rev. **142**, 519 (1966).

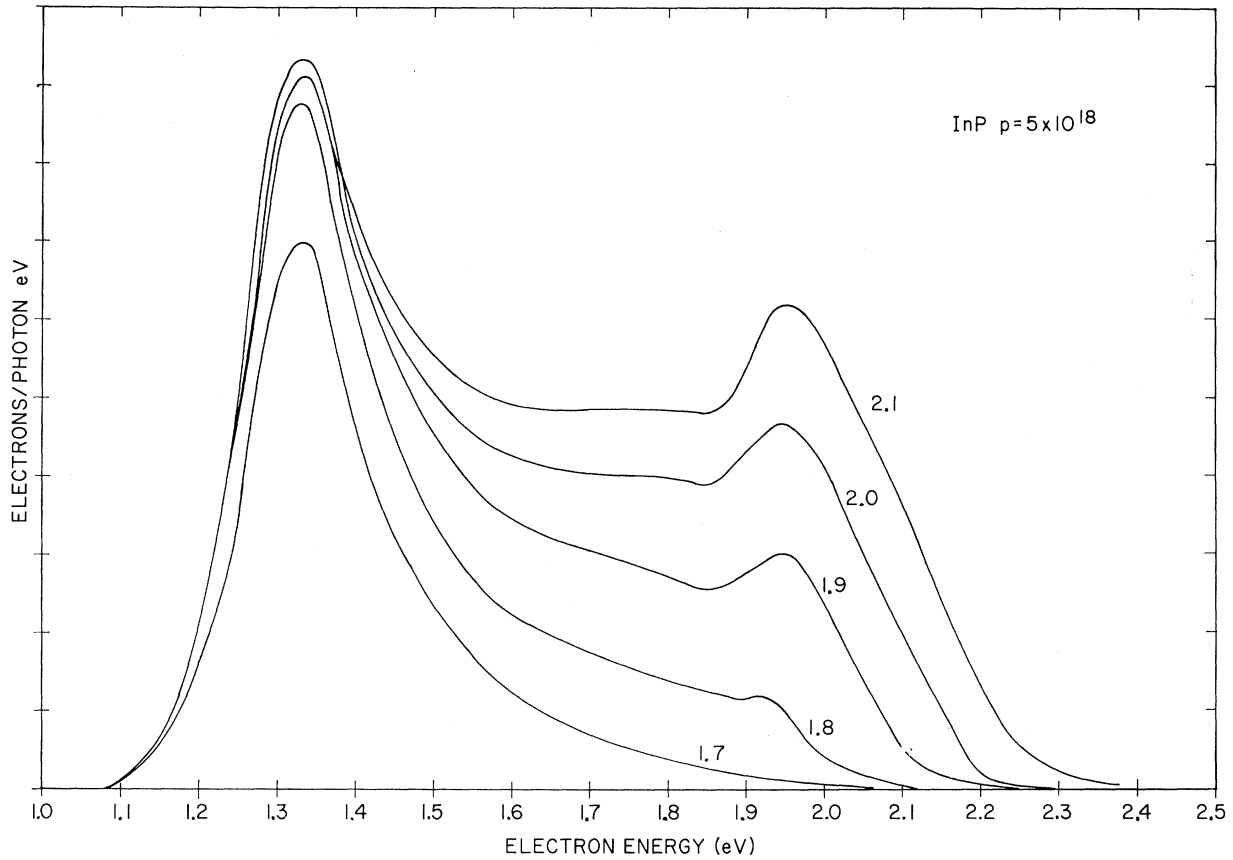


FIG. 2. Normalized and smoothed experimental energy-distribution curves for a $5 \times 10^{18} \text{ cm}^{-3}$ Zn-doped InP crystal with a Cs_2O surface layer shown every 0.1 eV for a photon energy range of 1.7–2.1 eV.

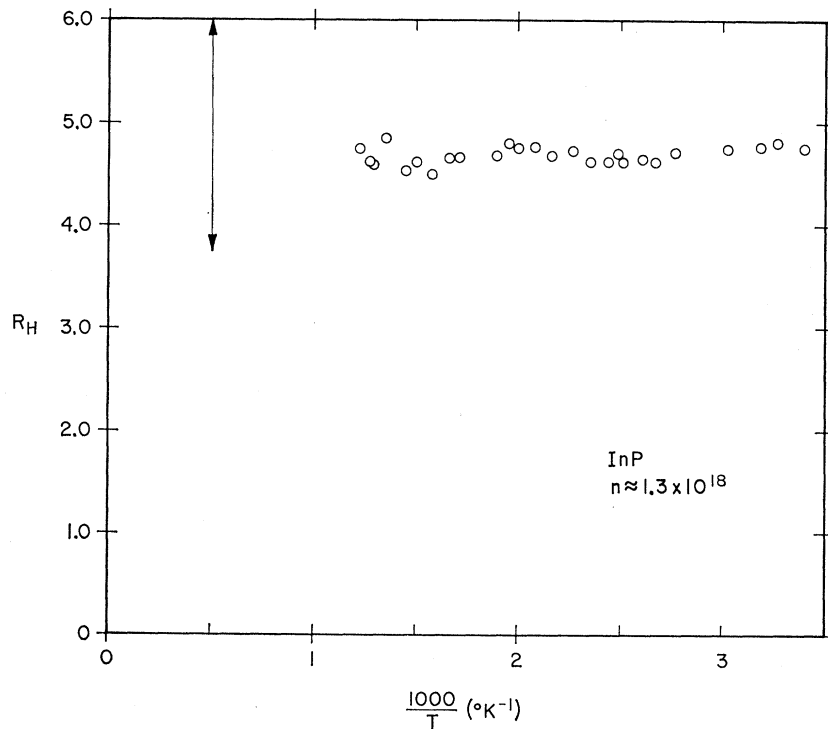


FIG. 3. Hall coefficient for *n*-type InP as a function of temperature. The constant Hall coefficient for temperatures up to 800°K implies that there are no minima within 0.5 eV of the Γ_1 minima. If there were, the Hall coefficient would fall outside the range indicated by the arrows at the higher temperatures.

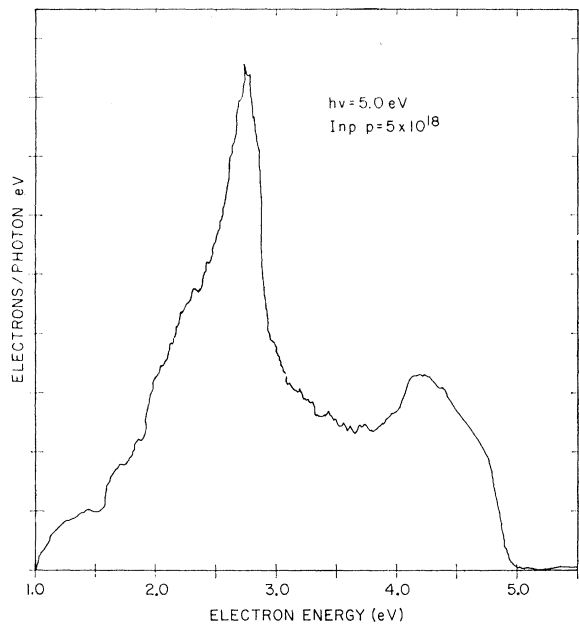


FIG. 4. Energy distribution curve for a photon energy of 5.0 eV, for the same crystal as Fig. 2.

The sample was cleaved at a pressure of $\approx 5 \times 10^{-11}$ Torr and treated with alternate exposures of Cs and O_2 until a peak yield (with white light) was obtained. This occurred at ≈ 2 Langmuirs (μ Torr sec) of total O_2 exposure. The crystal was then moved inside a spherical collector can where the EDC measurements were made using the ac retarding potential method.² The monochromator used had a resolution of $\pm 60 \text{ \AA}$ ($\pm 0.02 \text{ eV}$ at 2.0 eV). Appropriate filters were used to reduce scattered light. Both a tungsten source and a mercury source were used to cover the desired energy range.

III. BAND-STRUCTURE INFORMATION OBTAINED FROM ENERGY-DISTRIBUTION CURVES

Figure 1 shows the approximate band structure of InP near the energy gap. For low photon energies such as shown at (a), all photoexcitation will be to states lower in energy than the upper valleys, and the electrons will thermalize in the Γ_1 minima. For higher photon energies, such as shown at (b), some excitation will be to energies large enough that scattering can

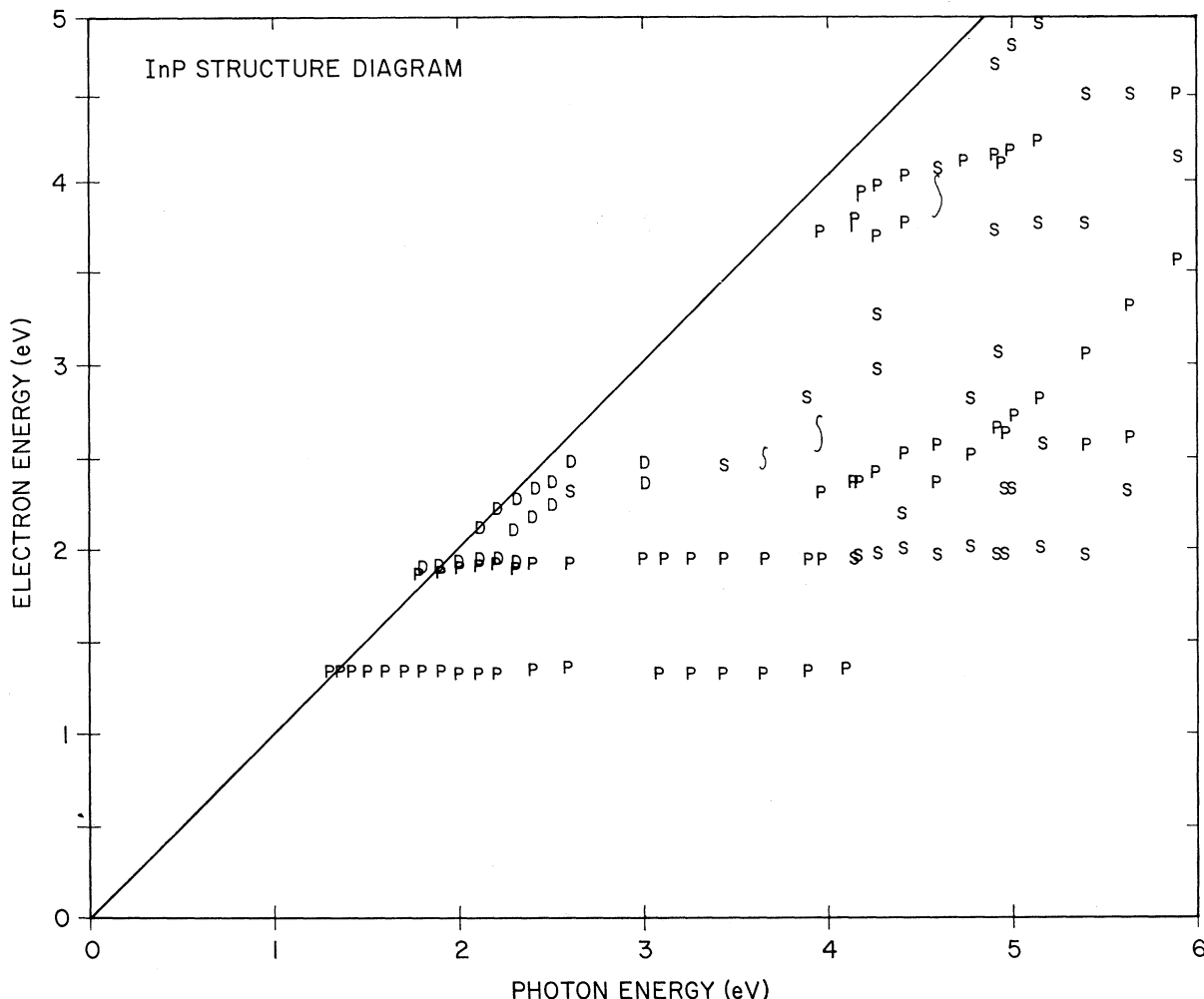


FIG. 5. Structure diagram showing the location of EDC structure for a 5×10^{18} Zn-doped InP crystal. Structures which are definite peaks are identified by (P). Shoulders on the EDC are identified with (S). The center of a Z-shaped structure on the derivative is identified by (D).

occur to the upper valleys and thermalization will take place there.

Figure 2 shows a series of normalized energy distribution curves taken over a photon energy range of 1.7–2.1 eV. There is clearly an upper valley at 1.95 eV, giving a lower-to-upper-valley separation $\Delta=0.61$ eV at room temperature. There are some electrons emitted in the energy range between the two valleys. However, high-temperature Hall measurements on *n*-type InP, shown in Fig. 3, indicate that there are no minima within 0.5 eV of the lowest minima (assuming an effective-mass ratio of 15 and a mobility ratio of 20 using the equations of Aukermann and Willardson⁸). Thus we are reasonably certain that the valleys at 1.95 eV are the next highest above the lowest (Γ_1) valley.

It is possible, using higher photon energies, to obtain additional information about the band structure further from the energy gap. For example, Fig. 4 shows an energy-distribution curve for a photon energy of 5.0 eV, where two definite peaks and several shoulders are visible. Data from these curves are conveniently plotted on a structure diagram,⁹ shown in Fig. 5, which plots the position of peaks (*P*), shoulders (*S*), and *Z*-shaped structures² on the derivative curves (*D*) as a function of photon energy. Horizontal lines of structure correspond to conduction-band minima. Slanting lines usually (in III-V semiconductors) correspond to a large region where a valence band and a conduction band are approximately parallel in two directions in the Brillouin zone.⁹

There are two possibilities for the band structure of InP which are consistent with these data. The minima at 1.95 eV could be either X_{1-} or L_{1-} -type minima (all known recent band-structure calculations agree that the minima are at the zone edge at *X* and *L*). An adjusted orthogonalized-plane-wave (OPW) band-structure calculation matched to the direct band gap, a 0.61-eV lower-to-upper-valley separation, and a 2.9-eV direct gap at *L* (assuming the gap at *L* is a few tenths of an eV less than the E_1 electroreflectivity peak¹⁰) gives the results shown in Fig. 6 as the dotted curve, with the 1.95-eV minima being at *X*. However, recent data from GaInP alloys^{11,12} indicate that the X_1 minima in InP are at 2.1–2.2 eV, meaning that the 1.95-eV minima observed here are L_1 -type. Recent

⁸ L. W. Aukermann and R. K. Willardson, *J. Appl. Phys.* **31**, 939 (1960).

⁹ W. E. Spicer and R. C. Eden, in *Proceedings of the International Conference on Semiconductors, Moscow, 1968* (unpublished), Vol. 1, p. 65.

¹⁰ M. Cardona, H. L. Shaklee, and F. H. Pollak, *Phys. Rev.* **154**, 696 (1967).

¹¹ M. P. Lorenz, W. Reuter, W. P. Dumke, R. J. Chicotka, G. D. Pettit, and J. M. Woodall, *Appl. Phys. Letters* **13**, 421 (1968).

¹² C. Hilsun and P. Porteous, in *Proceedings of the International Conference on Semiconductors, 1968* (unpublished), Vol. 2, p. 1214.

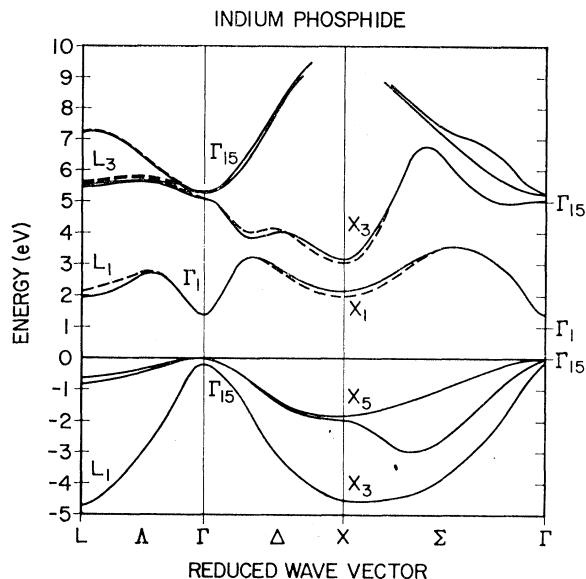


FIG. 6. Two possible band structures for InP. The dotted curve is an adjusted OPW calculation matched to the bandgap, the E_1 and $E_1+\Delta_1$ electroreflectivity peaks (Ref. 10), and a 0.61-eV lower-to-upper-valley separation. The solid curve is a modification of the calculated band structure which is consistent with Refs. 11–13 as well as the current data, and probably represents the correct form of the InP band structure.

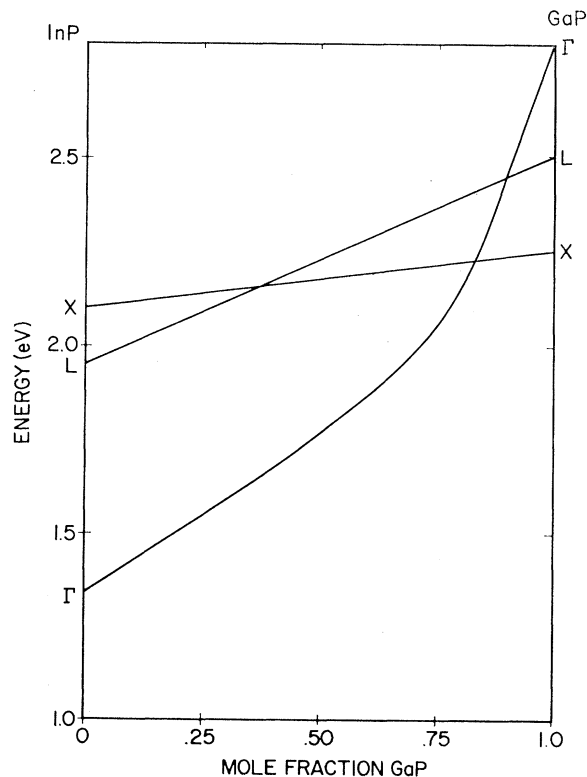


FIG. 7. Location of the three lowest conduction-band minima in the GaInP ternary, consistent with Refs. 11–13 and the current data.

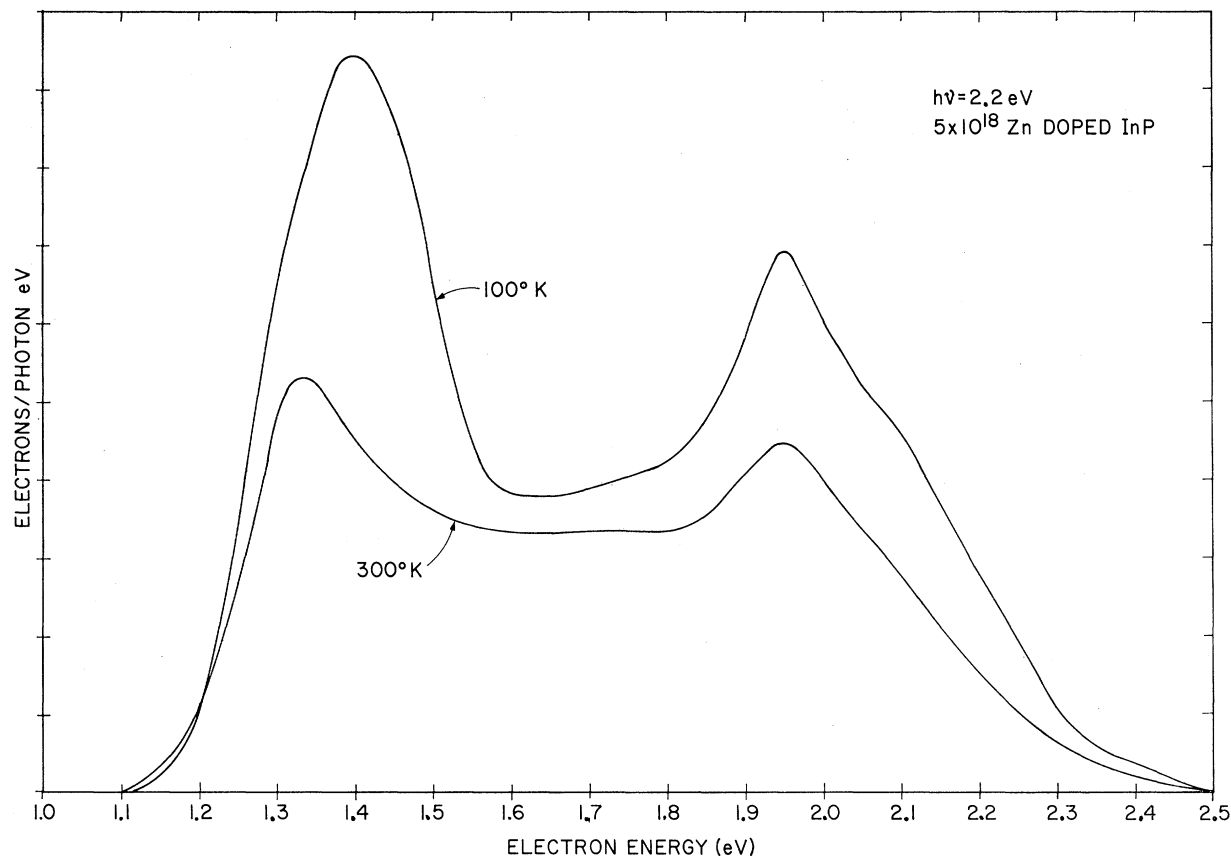


FIG. 8. EDC's for a photon energy of 2.2 eV, taken at 100 and 300°K crystal temperature.

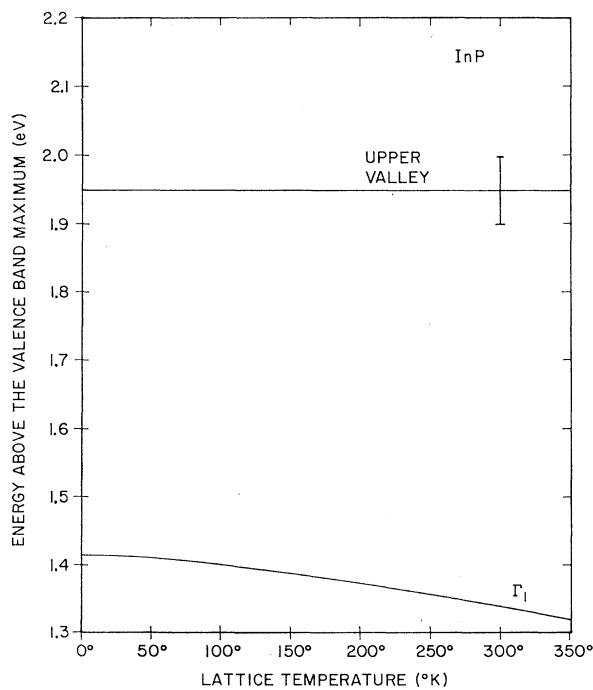


FIG. 9. Temperature dependence of the upper and lower-valley positions in InP.

electroreflectance data¹³ on $\text{InAs}_{1-x}\text{P}_x$ alloys gives strong evidence that the Λ transition responsible for the E_1 and $E_1 + \Delta_1$ peaks moves away from the L_1 point toward Γ for increasing x . Thus, the direct gap at L can easily be several tenths of an eV less than the E_1 peak, consistent with the placing of L_1 at 1.95 eV. If this is the case, the L_1 minima would not be seen in bandgap measurements anywhere across the GaInP alloy series, as shown in Fig. 7. The solid curve is a modification of an adjusted OPW calculation setting $\Gamma_1 = 1.34$ eV, $X_1 = 2.1$ eV, and $L_1 = 1.95$ eV. Based on the interpretation of the GaInP and the InAsP results, the solid curve very probably represents the correct form of the InP band structure.

TABLE I. Parameters used in the calculation.

$\theta = \hbar\omega_{\text{opt}}/k = 480^\circ\text{K}$
$m_{\Gamma}^* = 0.06m_0$
$(1/\epsilon_\infty) - (1/\epsilon_0) = 0.024$
(low-field mobility = 5500 cm^2/Vsec)
density-of-states ratio = 40
upper-valley mobility = same as X_1 in GaAs
$n = 10^{14} \text{ cm}^{-3}$
$\tau_{\Gamma U} < \tau_{\Gamma\Gamma'}$ for $E > E_U$, where U is the upper valley

¹³ A. G. Thompson, J. E. Rowe, and M. Rubenstein, J. Appl. Phys. **40**, 3280 (1969).

FIG. 10. Velocity-field characteristic for InP, compared with the GaAs characteristic.

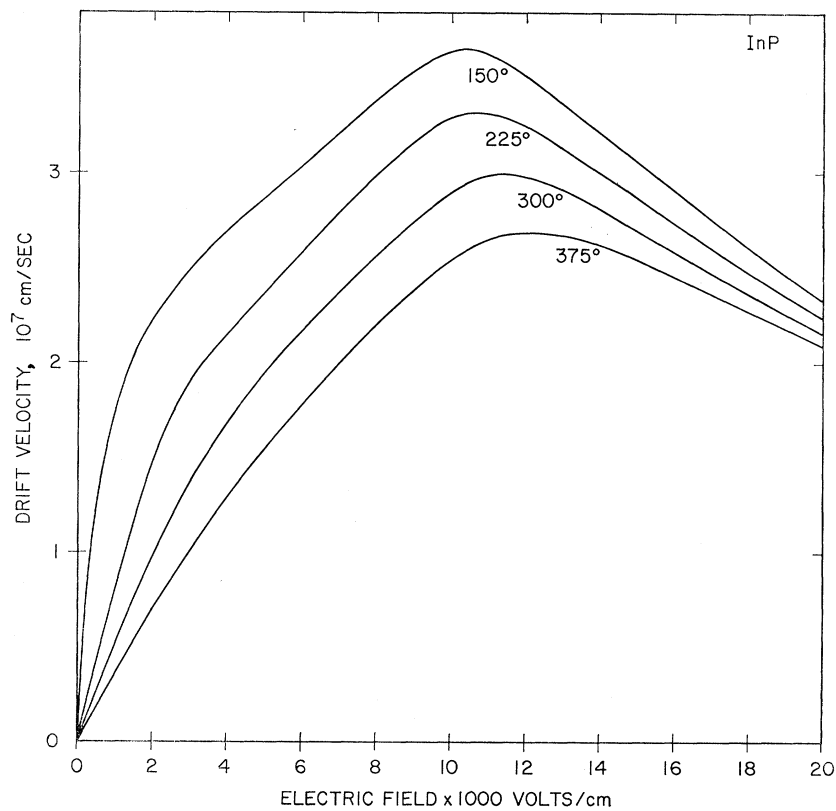
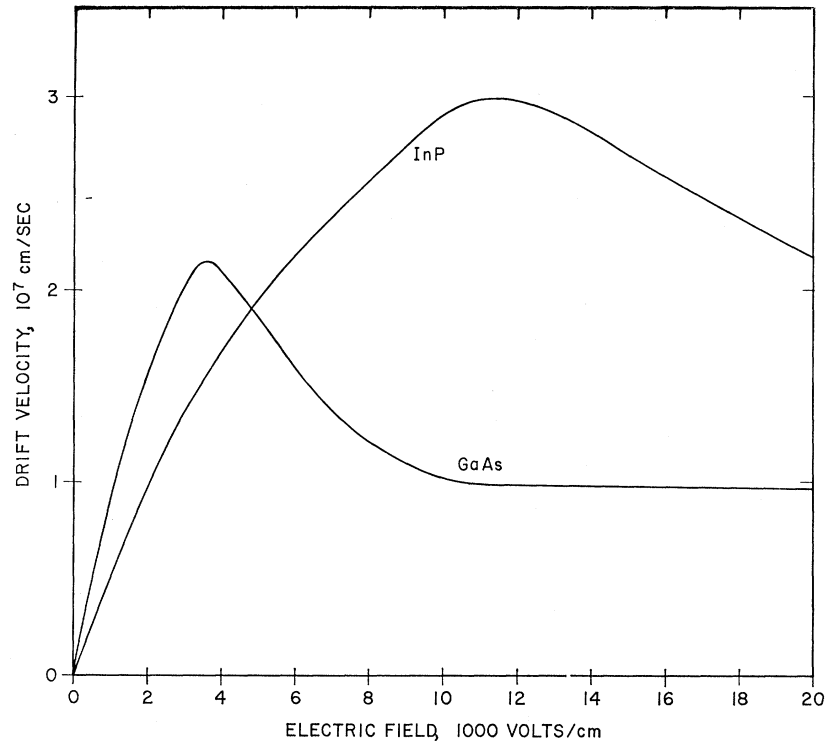


FIG. 11. Temperature dependence of the InP velocity-field characteristic.

The conduction-band minima below Γ_{15} (in the $\Gamma-X$ direction) is seen clearly in Fig. 5 as the horizontal series of peaks and shoulders around an electron energy of 3.8 eV. The lowest photon energy peak in this series is only a few tenths of an eV below the $E=h\nu$ line, demonstrating that the initial state involved is near Γ in the valence band.

IV. TEMPERATURE DEPENDENCE OF INTER-VALLEY ENERGY SEPARATION

By observing photoemission from a cooled sample, it is possible to trace the temperature dependence of the valley positions. Figure 8 shows two EDC's for a photon energy of 2.2 eV, taken at crystal temperatures of 100 and 300°K. Figure 9 shows the resultant temperature dependence of the upper- and lower-valley positions, assuming a square-law variation with temperature. The upper valley does not move, within the limits of experimental accuracy.

V. VELOCITY-FIELD CHARACTERISTIC

The energy separation between upper and lower valleys is one of the most important parameters in determining the velocity-field characteristic. A velocity-field calculation for InP has been done using the energy separation shown in Fig. 9, following the calculation of Harris and James¹⁴ on GaAs and GaAsP. The

¹⁴ J. S. Harris and L. W. James (unpublished).

parameters used in the calculation are shown in Table I. The calculation includes impurity scattering, optical photon scattering, and nonparabolicity of the lower valley according to Kane's¹⁵ theory. The correct parameters for determining the upper-valley mobility are not presently available. The values appropriate for X_1 in GaAs are used as an approximation. Changes in these values would be reflected principally in the value of the negative differential mobility and in the valley velocity (which is not predicted here). The results of the calculation are shown in Fig. 10, compared with the GaAs characteristic calculated using the same program.¹⁴ InP has a higher peak drift velocity and a much higher threshold field for negative differential mobility. Gunn's original measurements of InP⁵ gave an average field at threshold of 7200 V/cm, but the actual threshold field could be higher, as predicted here (11 500 V/cm), due to nonuniform doping in Gunn's sample. Figure 11 shows the calculated InP velocity-field characteristic for a range of lattice temperatures.

ACKNOWLEDGMENTS

The authors wish to thank C. Hilsum and J. S. Harris for many helpful discussions. They also thank Forest B. Williams of Monsanto Research for supplying the InP crystal.

¹⁵ E. O. Kane, J. Phys. Chem. Solids 1, 249 (1957).